# Approaches to Uncertainty Visualization

Alex T. Pang, Craig M. Wittenbrink*, and Suresh K. Lodha
Computer Science Department
University of California
Santa Cruz, CA 95064, USA
*Hewlett-Packard Laboratories
1501 Page Mill Road, Palo Alto, CA 94304, USA

September 6, 1996

**Abstract**

Visualized data often have dubious origins and quality. Different forms of uncertainty and errors are also introduced as the data are derived, transformed, interpolated, and finally rendered. In the absence of integrated presentation of data and uncertainty, the analysis of the visualization is incomplete at best and often leads to inaccurate or incorrect conclusions. This paper surveys techniques for presenting data together with uncertainty. These uncertainty visualization techniques present data in such a manner that users are made aware of the locations and degree of uncertainties in their data so as to make more informed analyses and decisions. The techniques include adding glyphs, adding geometry, modifying geometry, modifying attributes, animation, sonification, and psycho-visual approaches. We present our results in uncertainty visualization for environmental visualization, surface interpolation, global illumination with radiosity, flow visualization, and figure animation. We also present a classification of the possibilities in uncertainty visualization, and locate our contributions within this classification.

**Keywords:** classification, comparative visualization, differences, data quality, verity.

# 1 Introduction

With few exceptions, most of the visualization research has ignored or separated the presentation of uncertainty from data. Part of the reason is the inherent difficulty in defining, characterizing, and controlling the uncertainty in the visualization process. Another reason is the lack of methods that present uncertainty and data. We have seen this as an opportunity for research with great potential in a wide variety of applications. Some examples are: comparative visualization of experimental and simulation data, quantitative and visual analysis of image compression algorithms, comparison of volume rendering algorithms and volumetric data sets, finite element analysis, data assimilation, ensemble forecasting, as well as those presented in this paper. The common underlying problem in these areas is visually mapping data and uncertainty together into a holistic view.

As a possible solution, one might consider setting free parameters to uncertainty values using existing surface, volume, flow, and multi-dimensional visualization methods [CBB91]. In fact, we do start with existing methods. However, even with the simple task of designing glyphs or icons that incorporate uncertainty information [Bri84, Tuf90, WPL96, MM94], the process is sometimes counter-intuitive. For example, while a glyph may appear appropriate by itself, the user's perception of the glyph may be different when a group of them is presented in various scales and locations. Thus, while some of the methods we have examined are not necessarily new,

1

they must be able to render and convey the data in complete accordance with the facts. This has been recognized and is often stated as a worthy goal in scientific visualization (e.g. in the IEEE Visualization discussions on *How to Lie with Visualization*, IEEE Visualization panels and reports [GU95], and the NCGIA initiative on *Visualization of Spatial Data Quality* [BBC91]), but it has rarely been pursued or realized. In our investigation of uncertainty visualization, our approach has been to look at the needs of different application areas and to develop methods to address them. We found that in many instances, applications are orthogonal to methods. That is, a method developed for an application may be applicable in other areas. At the same time, an application may provide ideas for a visualization method that may not have been apparent without the application context. A simple example would be animation as a means to convey uncertainty information, and developing uncertainty visualization methods for comparing modeled versus motion-captured animation data. Because of this synergy, new applications provide ideas for more methods. The methods presented here represent significant steps toward achieving the goals of uncertainty visualization.

This paper is organized as follows: section 1.1 defines uncertainty visualization, and identifies the different sources of uncertainty; section 2 classifies methods for uncertainty visualization ; section 3 presents our new uncertainty visualization methods; we then conclude this paper with some more ideas for applications and methods of uncertainty visualization.

## 1.1   What is Uncertainty Visualization?

Uncertainty visualization strives to present data together with auxiliary uncertainty information. These visualizations present a more complete and accurate rendition of data for users to analyze. The methods employed in uncertainty visualization may range from *overloading* of visual parameters such as those commonly found in multivariate visualization, to *verity* visualization [WPL95, WPL96] where the display of both data and uncertainty is inseparable within the same picture. Applications which can benefit from uncertainty visualization are those where there is a chance for uncertainty to be introduced in the visualization process, and where such uncertainty matters. Depending on the intent or purpose of the visualization, these uncertainty information may be presented in a subdued manner to serve as a subtle reminder of the presence of uncertainty to the users; or these uncertainty information may be highlighted and even exaggerated to help in data comparison tasks. The ultimate goal of uncertainty visualization is to provide users with visualizations that incorporate and reflect uncertainty information to aid in data analysis and decision making.

## 1.2   What is Uncertainty?

We define uncertainty to include statistical variations or spread, errors and differences, minimum-maximum range values, noisy, or missing data. This broad umbrella is intended to capture most if not all the possible types and sources of uncertainty in data. NIST has written a standards report [TK93] which identifies four ways of expressing uncertainty. For the discussion in this paper, we consider three types of uncertainty: *statistical* – either given by the estimated mean and standard deviation, which can be used to calculate a confidence interval, or an actual distribution of the data; *error* – a difference, or an absolute valued error among estimates of the data, or between a known correct datum and an estimate; and *range* – an interval in which the data must exist, but which cannot be quantified into either the statistical or error definitions. Note that the term data quality has an inverse relationship with data uncertainty [PFN94] and hence can also take advantage of the techniques presented in this paper.

## 1.3   Sources of Uncertainty

In order to understand what is overlooked in visualization, we quickly review the sources of uncertainty, errors, and ranges within data. Fig. 1 illustrates the three major blocks in a visualization pipeline leading to the analysis of the visualization output. It is clear that different

forms of uncertainty are introduced into the pipeline as data are acquired, transformed, and visualized.
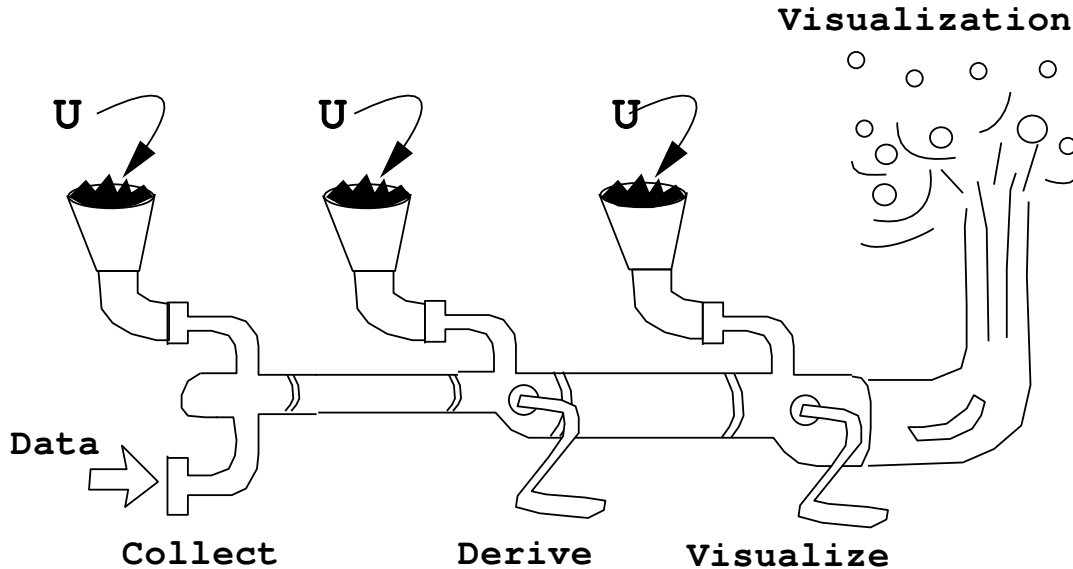
**Visualization**



Figure 1: This visualization pipeline shows the introduction of data uncertainty from models and measurements, derived uncertainty from transformation processes, and visualization uncertainty from the visualization process itself.

**Uncertainty in acquisition:**

Starting with the data acquisition stage, one will note that nearly all data sets, whether from instrument measurements, numerical models, or data entry have a statistical variation [Cha83]. With instruments, there is an experimental variability whether the measurements are taken by a machine or by a scientist. The more times the measurement is taken, the more confident the measurement. But there will be a statistical variation in these measurements. The same is true for data from numerical models and human observations or inputs. In numerical modeling, the model and its parameters have been decided by a domain specialist, and are inherently a simplification (e.g. linearization of a nonlinear system) of the system being modeled. In addition to model simplification and sensitivity of these models to input parameters, numerical calculations performed on these models also introduce errors due to the choice of integration algorithms and the limited precision of the computing machinery. Likewise, there is variability in human observations both in terms of difference in perception among individuals and also to slight differences when asked to perform a task repeatedly.

**Uncertainty in transformation:**

Often times, raw data are not rendered directly but are first subjected to further transformations with or without the knowledge of the person doing the visualization task. These data transformation operations may be as simple as conversion from one unit of measure to another, or may involve some algorithm to fuse one or more types of data together to derive a new data type. Data transformation operations may occur as early as the data acquisition stage or later in the visualization stage. Likewise, data may be rescaled, resampled, quantized, etc. either prior to, or as part of, the visualization stage. The key point is that these transformations alter the data from its original form, and have the potential of introducing some uncertainty.

**Uncertainty in visualization:**

What is more interesting and perhaps not self evident is that uncertainty is also introduced in the visualization stage itself. For instance, in global illumination of 3D scenes, radiosity algorithms use approximations for calculating form factors. Some recent work in this area addressed the issue of controlling the errors [GK94, LSG94, ATS94]. As these researchers also pointed out, the rendering process introduces uncertainty arising from the data collection process, algorithmic errors, and computational accuracy and precision. Similarly, there are different approaches to direct volume rendering of 3D data sets [UH90, MMMY96] resulting in slightly different renderings of the same data set. The differences in the resulting images may be due to different ray traversal methods or the different filter functions used in splatting; or they may be due to tetrahedralization or resampling processes; or they may be simply due to the tradeoffs between speed and image quality.

Uncertainty introduced in the visualization process is not limited to radiosity and volume rendering, but are also present in more routine operations. For example, the use of interpolation is quite prevalent in taking slices through data sets, in contouring, as well as isosurface algorithms [LC87, VGW94], to name a few. Surface approximation and interpolation is used in dealing with scattered data sets [Lod96]. Here, a variety of tradeoffs exist in performance and accuracy, and there is no ideal surface in many cases because of the many free parameters available [Far88, LSPW96]. In many cases, the data that are to be interpolated have numerous errors, and may even lack topology information [HDD+94].

Similar difficulties and range of choices produce uncertainty in flow visualization methods. For example, different integration methods, step sizes, orders, and seeding strategies lead to slightly different flow visualization results. Effects of uncertainty are more pronounced in the vicinity of or on critical points in the flow field. These differences may at times result in drastically different flow visualizations [DH96].

Animation allows visualization to include an additional parameter, usually time. Again, there are several opportunities for uncertainty to be introduced. The process of in-betweening to fill in frames between key frames is analogous to surface interpolation, and though no method is correct, there are many methods available, and all of them will result in slight variations. Aside from differences arising from interpolation of positional information, potentially more serious differences may arise from interpolation of orientation information depending on whether quaternions or Euler angles are used.

While we have tried to identify the common and major culprits of how uncertainty are introduced in the visualization pipeline, this is by no means an exhaustive list. Hopefully, this quick enumeration will draw the attention of visualization designers and users to the potential pitfalls of blindly using visualization methods without fully understanding the limitations and assumptions of each method. We next turn our attention to classifying visualization approaches, then uncertainty visualization approaches, and finally presenting several new methods for uncertainty visualization.

## 2    Classification of Methods

To classify uncertainty visualization approaches, we first consider more general classifications. Keller and Keller [KK93] classify visualization by using a taxonomy of visualization goals. Tufte [Tuf83] classifies visualizations by developing evaluation and analysis methods such as data-ink maximization. Carswell [Car92] and Cleveland [Cle85, CM86] use evaluation as a basis for the theory of specifiers, that fundamental parameters, length, area, ratios, etc. describe and determine the effectiveness of visualization. Bergeron and Grinstein [BG89] introduce a classification that uses lattice arrangements of data. Brodlie [BCE+92] describes a classification based on the dimensionality of the entity that is being visualized. Application specific visualization classifications have been done by Hesselink et al. [HPvW94] for vector and tensor field visualization.

We create a classification system that is similar to the systems of Brodlie and Hesselink et al. in certain aspects, but is extended to accommodate uncertainty visualization techniques. Brodlie classifies techniques using two characteristics. First, he uses the *underlying field*, where data may

be grouped as dependent or independent variables, and classified as having ordinal or nominal values. Second, he uses the *view*, which is an operation on the underlying field to produce a pictorial representation. For example, generating a set of contour lines for a given height field, or generating the surface representation of the height field. Hesselink et al. classify techniques using three characteristics. First, they use the *order* of the data: scalar, vector, or tensor (three data orders). Second, they use the spatial *domain* of the visualization objects: point, line, surface, or volume (four domains). Third, they introduce the *information level* of the data: elementary, local, and global (three information levels). However, these classifications do not account for different types of uncertainty information or techniques. In order to incorporate uncertainty information into visualization schemes, we propose a classification with five characteristics: *value, location, data extent, visualization extent*, and *axes mapping*. Each of these concepts are defined below.

1. *Value* of datum and its associated value uncertainty (scalar, vector, tensor, multivariate). The data value, $y$, may be characterized as a scalar, a vector, a tensor or a multivariate variable. A multivariate variable has several components, each of which can be a scalar, a vector or a tensor. In our classification scheme, *value* includes possible uncertainties associated with each data value. For example, $y = [y_1, y_2, ..., y_m]$ can be used to represent data values that are multi-valued scalars, vectors, or tensors. Likewise, $U_y = [u_{y_1}, u_{y_2}, ..., u_{y_m}]$ can be used to represent corresponding uncertainties in data value. Value corresponds to the dependent variables of Brodlie's underlying field and the order of Hesselink et al.

2. *Location* of datum and its associated positional uncertainty (0D, 1D, 2D, 3D, time, etc.). This characteristic identifies the dimensionality of the space in which the data resides. It specifies how many independent variables are used to describe each data value. For example, 0D ,1D, ... nD and time. In our classification scheme, this description is extended to include positional uncertainty. For example, if an n-dimensional datum has a value $y$, it can be specified as $y = f(x_1, x_2, ..., x_n)$, while its corresponding positional uncertainty may be specified by $U_x = [u_{x_1}, u_{x_2}, ..., u_{x_n}]$. Location corresponds to the independent variables of Brodlie's underlying field.

3. *Extent* of datum location and value (discrete or continuous).
The *data extent* corresponds to the distribution, range, interval, or period over which data is valid. For example, if a highly fluctuating variable such as wind velocity was measured and averaged over time, the time window would specify the time extent (extent of location); the distribution of wind readings and the range of wind readings over this time period would specify the velocity extent (extent of value). On the other hand, extent may also be used to specify an interval of acceptable values (e.g. 0 ... 255) for each datum. That is, value extent of $y$ can be expressed as $E_y = [e_{y_1}, e_{y_2}, ..., e_{y_m}]$, where each $e_{y_i}$ can be an interval or a distribution defined over the location extent $E_x = [e_{x_1}, e_{x_2}, ..., e_{x_n}]$, where the location extent itself can be a range or distribution or some more complicated function of the data location. Varying data extents are common for sampled medical data in terms of the sample spacing, and common in environmental data in terms of the time averaging involved. For our purposes, we distinguish between two types of data extents – discrete and continuous. A discrete extent implies that data are valid at discrete domain values only, while a continuous extent implies data are valid through a continuous domain. An example of a discrete data extent is the population count associated with U.S. cities, while an example of a continuous data extent is the surface of the earth – where population can also be represented. Data extent corresponds roughly to the information level of Hesselink et al.

4. *Visualization extent* (discrete or continuous).
The visualization primitive extent determines whether individual datums are indicated or whether a continuous range of data are indicated. The visualization extents are grouped into discrete (includes points and glyphs) and continuous (includes curves, surfaces, volumes). Animation is orthogonal to these two. That is, animation can be used with both

discrete or continuous visualization extents. The choice of the visualization primitive extent is independent of the actual underlying extent of the data. For example, fitting a continuous line through a plot of heights of students in a class is a continuous visualization extent of a discrete data set. The data extent is independent of the visualization extent, though some mappings are more natural and useful than others. It is important to note that discrete visualization extents, such as glyphs, can be used with continuous data, and that continuous visualization extents such as parallel coordinate display [Ins85, ID90] can be used with discrete data. Visualization extent corresponds with views of Brodlie and domain of Hesselink et al.

5. *Axes mapping* defines visualization mapping (experiential or abstract).

It allows different variables or grouping of variables to be mapped together or to different axes. For example, one can use data values in place of location values for coordinate axes such as in a scatter plot, in order to investigate cause and effect relationships; or investigate the location using a spatial plot with the dependent variable(s) being visualized; humidity and temperature values can be treated as vector components; etc. Axes mapping allows two basic approaches to visualization: experiential rendering is to replicate the viewer's experience with the visualized phenomenon. Abstract rendering is to plot the data in a non-experience based mapping, which may result in additional insight and understanding. Both these visualization approaches may be used for uncertainty visualization to show what the true variations in the mapped axes are. Essentially, in multi-valued data sets, some projection of the n-dimensional data set must be used to produce a typically 2-dimensional visualization, perhaps over time, and there is considerable flexibility in the mapping beyond the experiential/abstract demarcation we use in this section.

| Value | Visualization Extent | |
|---|---|---|
| | discrete | continuous |
| scalar | glyphs (error bars, box plots, Tufte quartile plots) | pseudo-coloring, difference images, side-by-side, contour lines, blinking |
| multivariate | Chernoff faces, scatter plots | side-by-side, difference images |
| vector | glyphs (modified tensor probes) | modified streamlines/ribbons/tubes, modified LIC |
| tensor | glyphs (modified tensor probes) | modified hyperstreamlines |

Table 1: Existing and likely uncertainty visualization techniques.

Table 1 uses two characteristics (value and visualization extent) to classify existing uncertainty visualization methods. The other characteristics explain and demarcate the space in which visualization methods can be classified. The methods provided in the table can be shared across the other characteristics where deemed appropriate. A complete table for all the five characteristics is hard to display in two dimensions. Therefore, for sake of simplicity of presentation, we have chosen the two most representative characteristics that separate methods. The listing of all of the characteristics is the complete classification, and must be used to quantify a given uncertainty visualization technique.

Table 1's upper left cell, contains the most thoroughly researched statistical visualization work: the visualization of a scalar value and its uncertainty, such as the median, quartiles, and outliers of a statistically evaluated variable. If visualized with a discrete visualization extent, the variety of statistical plotting tools is impressive, including glyphs, with various attributes set to denote values, where attributes are the shape, color, etc. of a graphical specifier. We discuss attributes in more details in Section 3. Error bars can show the range of the data, and represent a glyph to show uncertainty that works well with the discrete visualization extent. A discrete

visualization extent can be formed either directly from discrete data, or densely sampled data that is sub-sampled, or continuous phenomena/data that is sub-sampled. The mapping of data makes it possible to visualize a given data set with many techniques, converting discrete data to continuous representation and vice versa.

Scalar data may also be visualized with methods that are continuous visualization extents, meaning they impart the effect that the phenomena is not discrete. For example, a discrete representation of data in a plot is to plot with points, while a continuous representation of those same points is to plot with a smoothly varying line that passes through the points. For this reason the scalar row, continuous visualization extent, cell in the upper right of the table, shows attributes of lines, contours, etc. to map the uncertainty to color or line style. Note, that the dimension of the data domain has not been chosen for the table, because higher dimensional domains have nice analogues, such as the transition from lines, to contours, to isosurfaces for 1D, 2D, and 3D.

The rest of the table shows those methods that deal with higher order data, including multivariate, vector, and tensors. A multivariate variable is simply a number, n, of scalar values that are to be simultaneously visualized, and encompasses the traditional multiple valued visualization methods, in addition to visualizing their uncertainty. Complex (real plus imaginary) data are typically handled with this approach as well. The vector is distinguished from the multivariate because it is less general, and there are data sets that are directly vector data sets. Flow visualization, wind, currents, etc. are of this type, and the assumptions in the visual mappings, and the techniques used are different than for the multivariate. Tensor uncertainty visualization takes the meaning of the multiple values and their uncertainty to be tensors. Because the most general method is the multivariate, vector and tensor data sets can use the multivariate methods. The reverse is also true, but the interpretation may not be correct, as in visualizing financial data as vectors. There are not many existing techniques for higher order data with continuous visualization extents. We now describe some existing uncertainty visualization methods and how they fit into our classification.

Many researchers are fully aware of the uncertainty, usually in the form of errors, in their data. These are usually displayed using some straightforward method such as side by side comparison or differencing. For example, Lischinski et al. [LSG94] used line plots to render uncertainty, Greene et al. [GK94] used difference images, and Arvo et al. [ATS94] used norms for the entire image. In surface interpolation, Hagen et al. [HHS$^+$92] used pseudo-coloring of the surface curvature and other properties of the surface. This is an example of scalar value (first row) continuous extent visualization (second column) in Table 1.

In geographic and information systems (GIS), researchers are aware of the statistical variation, and have employed a range of techniques to display this information. For example, aside from pseudo-coloring areas of maps to represent value uncertainty, they may also use contour lines to indicate regions of similar confidence levels. For cartographers, the contours may be for areas of similar spatial distortions from projections. Fisher [Fis94] proposed animation techniques such as blinking data points to represent data uncertainty. Gershon [Ger92] proposed animation for the display of uncertainty in fuzzily classified regions. These are examples of scalar value (first row) continuous visualization extent (second column).

We have not seen any visualization methods designed for presenting uncertainty information for vector or tensor data. However, some existing vector and tensor visualization methods can be modified to include uncertainty information. For example, tensor probes [dLvW93] with discrete visualization extents can be easily modified to incorporate uncertainty information. For continuous visualization extents, line integral convolution (LIC) [FC95] can use the uncertainty information to modulate the texture. Likewise, adding more variables into existing flow visualization methods such as streamlines result in streamballs [BHR$^+$94], and to hyperstreamlines [DH93] as well.

The taxonomy of existing methods of displaying uncertainty are summarized in Table 2. Our classification of uncertainty visualization techniques demonstrates that only the scalar value discrete visualization extent, or upper left entry in Table 1 has been adequately explored, where

the uncertainty may be shown with economy using Tukey's box plots [Tuk77], Tufte's quartile plots [Tuf83] and/or Cleveland's framed rectangles [Cle85]. What we describe in the following section are new methods for displaying higher dimensional uncertainty (e.g. a vector of uncertainty parameters) in surfaces and in animation applications. The primary methods we discuss are adding glyphs (Section 3.1), adding geometry (Section 3.2), geometry modification (Section 3.3), attribute modification (Section 3.4), animation (Section 3.5), sonification (Section 3.6), and psycho-visual approaches (Section 3.7).

| Technique | Value | Location | Data extent | Vis extent | Axes mapping |
|---|---|---|---|---|---|
| side-by-side | any | 2D or 3D | any | any | experiential |
| difference image | scalar | 2D, 3D, or time | any | continuous | experiential |
| pseudo-color | scalar | 2D or 3D | any | any | experiential |
| contour lines | scalar | 2D | any | continuous | experiential |
| blinking | scalar | 2D | any | any | experiential |
| scatter plot | multivariate | nD | any | discrete | abstract |

Table 2: Taxonomy of some existing uncertainty visualization methods as used in different applications

# 3    Uncertainty Visualization Methods

We have developed a variety of new uncertainty visualization methods. These are organized into a table showing general approach versus application domain (Table 3), as well as their classification according to the five characteristics listed in the previous section (Table 4). Entries in Table 3 indicate methods that can be used for an application. The presentation below is organized by general approach, with detailed description of how a particular method and its relationship to our classification scheme in Table 1. But first, we describe the four different applications that we have investigated, focusing on their relevance to uncertainty visualization and the type of uncertainty in each case.

| Approach | Application | | | |
|---|---|---|---|---|
| | Radiosity | Animation | Interpolation | Flow |
| Add glyphs | spherical | ladders | uncertainty | ellipsoidal |
| Add geometry | | snow angels | fat surfaces, bumps | ribbons |
| Modify geometry | affine transform | | IFS, displacement | |
| Modify attributes | reflectivity, textures | bump mapping | pseudo-color | |
| Animation | magnitude, frequency | oscillate | oscillate | batons, ranking |
| Sonification | | | pitch, instrument | duration |
| Psycho-Visual | left/right | | subliminal | |

Table 3: Some uncertainty visualization methods for a range of applications

**Radiosity:**

There are several motivations for comparing results from different radiosity algorithms. The main motivation is that, like direct volume rendering, radiosity calculations can be expensive and hence numerous works in this area have focused on different approximations to speed up the calculations. Competing results are often displayed side by side and the burden is placed on the user to identify the regions and extent of difference. Since rendering is an integral part

of the visualization process, we need to understand how these different forms of approximation influence the final picture. Another motivation for this application is its similarity to other applications. That is, radiosity is concerned with calculation of surface radiosities of a static 3D scene. The ability to highlight differences between competing methods on these surfaces can benefit other applications such as finite element analyses of structural components.

**Animation:**

In this particular application, we are interested in comparing two sets of animation data: modeled human motion versus motion-captured human motion. Positional data are available for key points of the body, such as head, hips, extremities, etc. However, the data could just as well be from other sources such as comparing animations using different interpolation methods, or from other applications such as different paths of streamlines in flow visualization. From a modeling point of view, it is important to understand how the modeled motions differ from actual human motions (or how one streamline is different from another streamline, etc.) in order to improve the animation model.

**Interpolation:**

In dealing with environmental data sets, one often encounters sparse and scattered data. The dispersion and sparsity of the data points are often attributed to the accessibility of the sites and the cost of the instruments that collect them. In an ideal situation, the field would be populated with enough instrumentation to sample the field at sufficient resolution to capture the phenomenon of interest. In reality, we have to approximate and/or interpolate the field based on the limited number of data points. Because the choice of interpolation algorithm can substantially influence the appearance of the interpolated field, it is important to understand how the distribution of data location as well as data values influence the performance of different algorithms.

**Flow visualization:**

There are several flow visualization software packages where users are given the option of selecting different integration methods, integration time interval, integration directions, etc. This flexibility may actually be detrimental if the user does not fully understand the impact of these choices on the resulting flow visualization.

Table 3 shows the four application areas discussed as columns, and a classification of uncertainty visualization methods along rows. We have split techniques into seven fundamental areas which provide a separation of means by which information are encoded into a visualization. The following sections describe each area and relate them to the applications.

## 3.1    Add Glyphs

A glyph is a geometrically plotted specifier that encodes data values. Glyphs encode information through their shape and/or color. An example would be arrow glyphs, which are used to visualize magnitude and directional information in vector fields. Glyphs can also be used to visualize uncertainty in a variety of ways. We have investigated glyphs in the following applications, radiosity [PF96], vector fields [WPL96, WSF$^+$95], surface interpolation [LSPW96], flow visualization [LPSW96], and key-framed animation [WPL95]. The primary issues in using glyphs for visualizing uncertainty are the sampling frequency/location and the placement orientation (e.g. [TB96]). For most of our applications to date, we have been able to specify the orientation through the nature of the data being presented. For example, in interpolation of a height field, there is going to be uncertainty in the heights, and the glyphs are therefore oriented vertically to indicate this height variation.

Glyphs in radiosity have included spheres whose radii are scaled to the difference in different radiosity solutions. For multivariate uncertainty information, ellipsoidal or more complicated

| Technique | Value | Location | Data extent | Vis extent | Axes mapping |
|---|---|---|---|---|---|
| material prop | scalar | 3D | discrete | surface | experiential |
| texture mapping | scalar | 3D | discrete | surface, volume | experiential |
| spherical | scalar | 3D | discrete | point | experiential |
| affine transform | scalar | 3D | discrete | surface | experiential |
| mag/freq | scalar | 3D | discrete | surface and anim | experiential |
| left/right | scalar | 3D | discrete | surface | experiential |
| bump mapping | multivariate | 2D and time | discrete | surface | experiential |
| snow angels | vector | 2D and time | discrete | surface | experiential |
| oscillation | multivariate | 2D and time | discrete | point, curve, anim | experiential |
| uncertainty glyph | vector | 1D or 2D | continuous | point | experiential |
| fat surfaces | scalar | 2D or 3D | continuous | surface, volume | experiential |
| IFS | multivariate | 1D, 2D, or 3D | discrete | continuous | experiential |
| displacement | scalar | 2D or 3D | continuous | surface | experiential |
| instrument | scalar | 1D | discrete | point | abstract |
| subliminal | nominal | 2D or 3D | discrete | surface | experiential |
| ellipsoidal | multivariate | 3D and time | continuous | point | experiential |
| ribbons | multivariate | 3D and time | continuous | surface | experiential |
| batons | multivariate | 3D and time | continuous | point, curve, anim | experiential |
| ranking | multivariate | 3D and time | continuous | curve and anim | experiential |
| duration | scalar | 1D or time | discrete | curve or anim | experiential |

Table 4: New uncertainty visualizations methods as applied to our applications

glyphs can be used together with color. Fig. 2 shows an example where the differences from two radiosity solutions are visualized with spherical glyphs.

Glyphs in vector fields have been custom designed to encode the magnitude and bearing uncertainties. We have worked with maximum likelihood output from ocean radars, wind sensing radars, and interpolated winds from scattered stations. Fig. 3 shows how uncertainty vector glyphs are used to visualize vector fields with derived magnitude and directional uncertainty information.

Glyphs in surface interpolation have been used to compare interpolants such as bilinear, multi-quadric, and Shepard's. The length of the glyph is scaled to the difference between the interpolants. Fig. 4 shows how such line glyphs do pairwise comparisons of the interpolated surfaces.

Glyphs in flow visualization have been used to show the deviation of flow solvers. Fig. 5 shows the use of glyphs to compare Eulerian integration versus Runge-Kutta, where the length of the glyph is the difference between two solvers.

Glyphs in key-framed animation have been used in a similar fashion to the flow visualization. They are used to illustrate path differences arising from using different interpolation methods.

The variety of applications that use glyphs for uncertainty visualization, as well as the variety of encodings possible with glyphs, make this method highly successful, and extensible to many other applications.

## 3.2    Add Geometry

Uncertainty can be visualized in certain applications by adding geometry to rendered scenes. While glyphs do add geometry, they are placed at discrete locations. Adding geometry is used to denote a more continuous representation of data. Techniques include contour lines, isosurfaces, streamlines, and swept surfaces and volumes. Some extensions of these techniques for uncertainty visualization are described below.
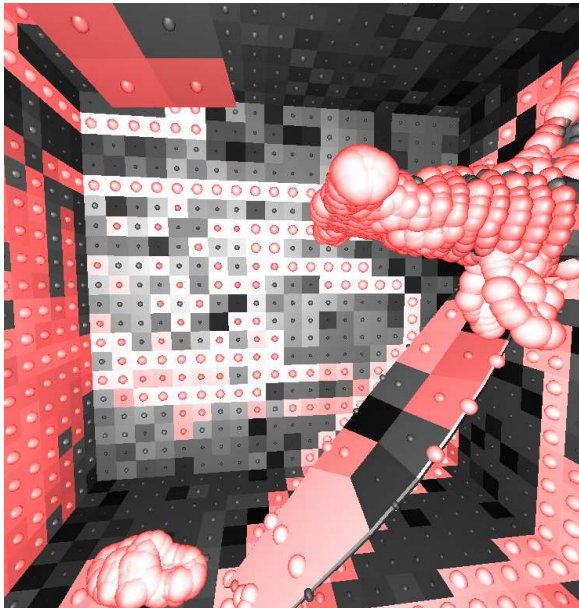
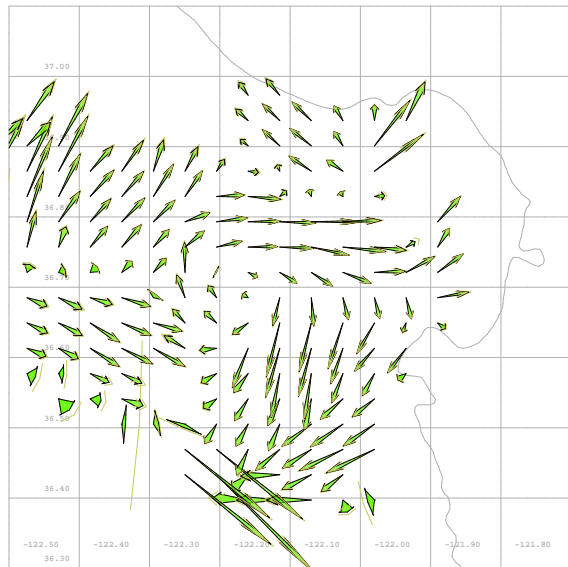Figure 2: Spherical glyphs scaled to radiosity differences.



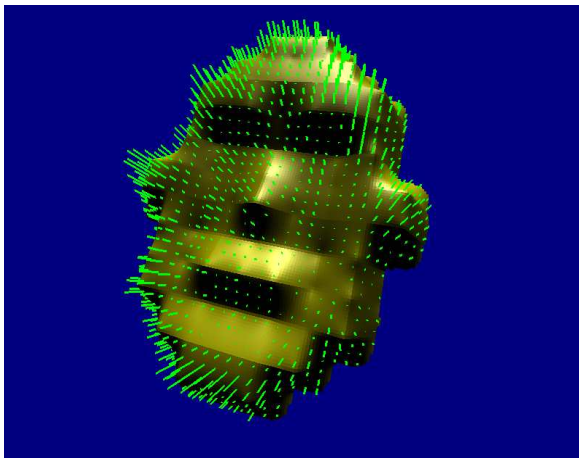Figure 3: Uncertainty vector glyphs over Monterey Bay.



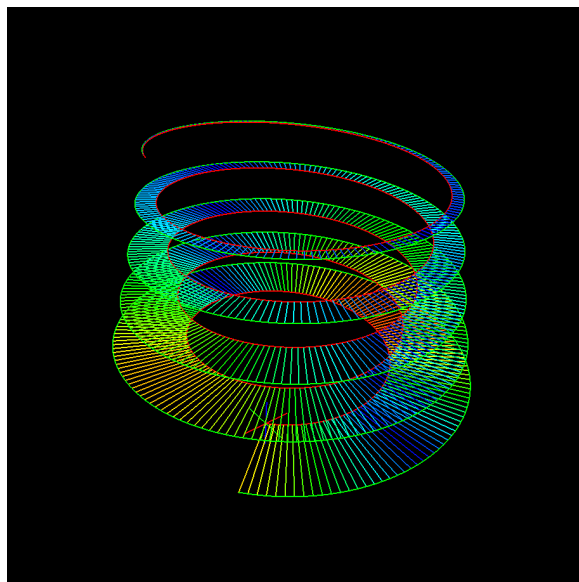Figure 4: Line glyphs show difference between bilinear and multi-quadric interpolated surfaces.



Figure 5: Line glyphs tile particle positions along streamlines computed by two different integration methods.

To show the differences between two methods of scattered data interpolation, a fat surface can be created by sweeping one surface to the other. This is illustrated in Fig. 6 where a cross sectional cut reveals varying thickness across the surface.
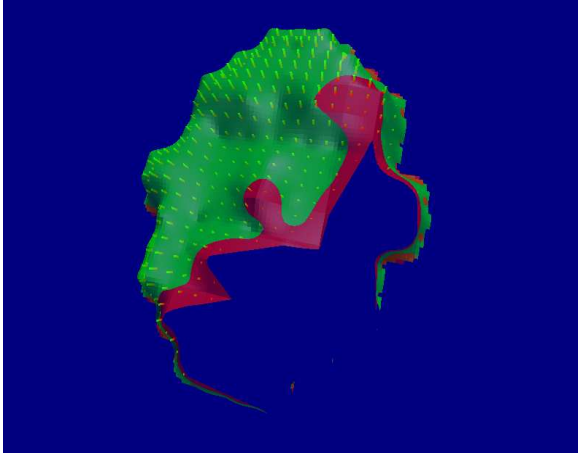


Figure 6: Fat surfaces showing the difference between the bilinear and multi-quadric interpolations. The cross sectional slice shows how fat surfaces can be used to exaggerate the difference.
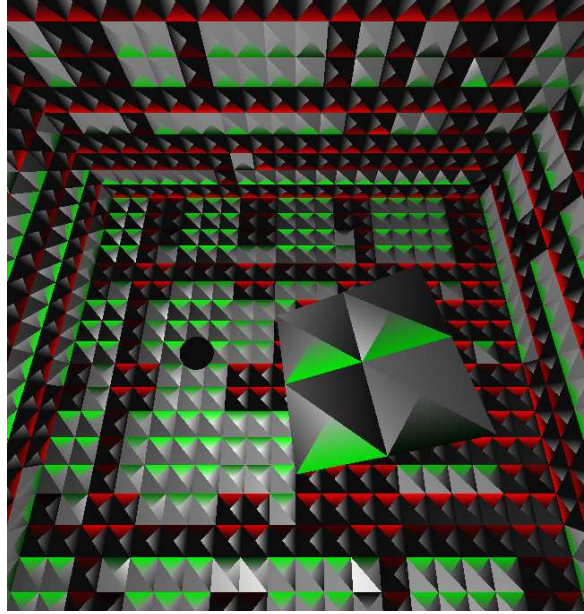


Figure 7: Surface patches are split into four pieces and displaced vertically according to radiosity differences.

Fig. 7 illustrates a variation where geometry is added on a per patch basis instead of over the entire region in order to show the radiosity differences on each patch. The patches are divided into 4 smaller patches and are displaced vertically at their centers by an amount proportional to the difference. Rather than displacing them up or down according to the signed difference, a red/green coloring scheme is used instead. Together with a movable light source (black sphere), the user can examine different areas in more detail.

For flow visualization applications, geometry is added in the form of uncertainty ribbons, representing the extent between two streamlines calculated from two different integration methods. See Fig. 8.

When comparing two sets of character animation, line segments are used to connect key points of the body. The area bordered by corresponding line segments of the simulated data and the motion-captured data are then used to sweep out an area on the same plane as the animation data. This is illustrated in Fig. 9 and is similar to having each stick figure do a snow angel one after the other over the same location. Regions which have less depression indicate more variance.

## 3.3   Modify Geometry

Uncertainty can be visualized by modifying geometry in a scene. Geometry may be translated, scaled, rotated, or generally warped or distorted. They may also be displaced, subdivided or refined.

Simple affine transformations, such as translation and rotation, have been used to indicate uncertainty in the data. For the radiosity application, the surface patches are either translated in or out according to the radiosity difference calculated by two different form factor methods (Fig. 10), or rotated up to a maximum of 90 degrees (Fig. 11).
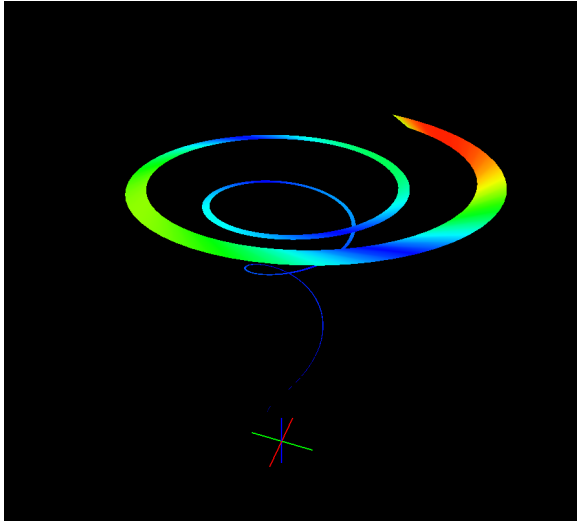
Figure 8: Uncertainty ribbons are used to show the deviations and twisting between two streamlines generated by different integration methods.
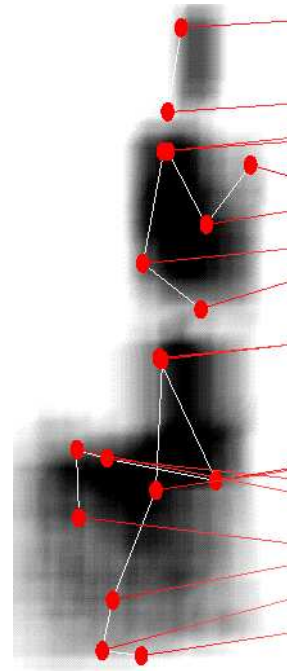


Figure 9: Snow angels are marks left on the ground by sweeping out limb segments. The amount of depression, which is mapped to gray level above, corresponds to the similarity in the two animation data sets.
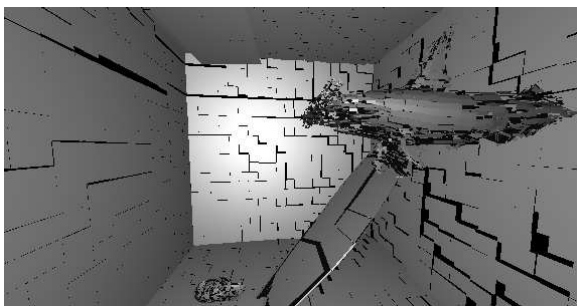


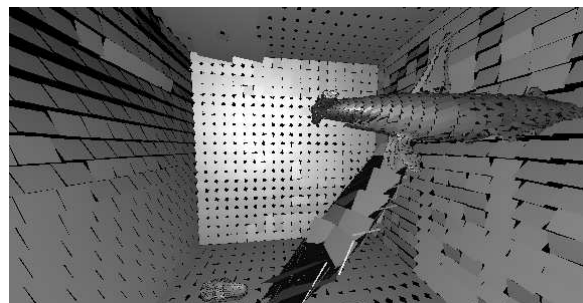Figure 10: Surfaces patches are translated in or out of their original positions to highlight differences.



Figure 11: Surfaces patches are rotated instead of translated giving a similar effect.

Fractal interpolation using iterated function systems (IFS) is an additional method we have used to impart uncertainty into the visualization. The interpolation method used in the reconstruction of sampled data sets during rendering impacts the interpretation of the data. We have found that smooth interpolations sometimes impart the message that the data itself represents a smooth phenomenon, or that there was a higher density of data collected than indicated. We developed interpolation methods to demonstrate uncertainty through the roughness of the surface or the variation in the volume [Wit95]. Fig. 12 shows a fractal interpolation of 2D scalar samples.

Similar to Fig. 12, Fig. 13 produces a bumpy looking surface. This is achieved by displacing the surface up or down according to the scaled difference between different surface reconstruction methods. The location and frequency of the bumps give an indication of the location and magnitude of deviation between the two methods of interpolation.
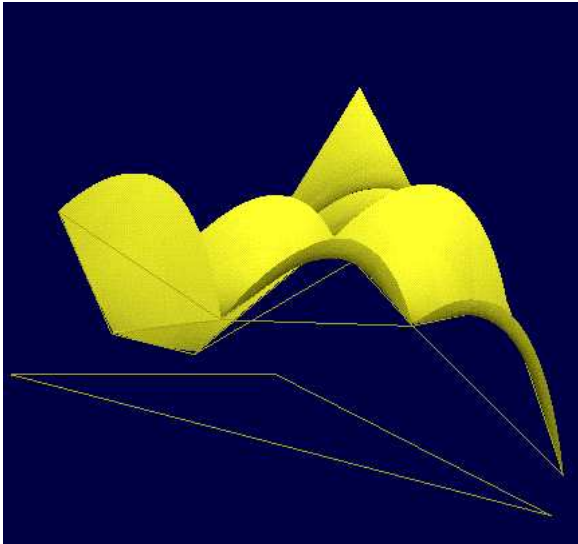
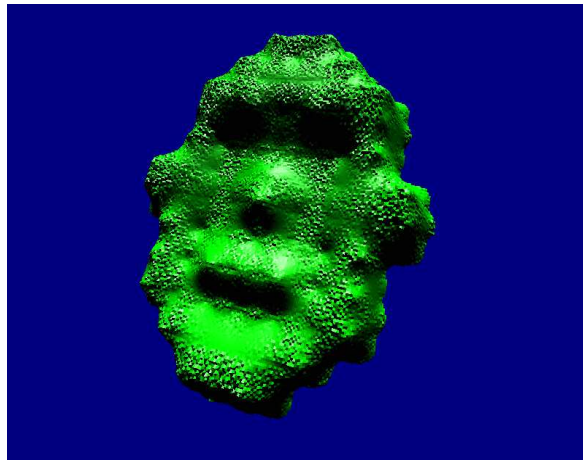

Figure 12: IFS surface interpolation of scattered data.



Figure 13: Bumpy looking surface created by simple facet displacement.

## 3.4    Modify Attributes

Uncertainty can be visualized by modifying attributes of geometry in the rendered scene. Attributes include the bidirectional reflectance distribution function (BRDF) and other means of controlling the shading such as pseudo-coloring. The control of the shading and coloring provides several parameters that can be mapped to uncertainty. The simplest is to use a color lookup table approach where a color palette is used to map uncertainty values to different colors on the visualization primitives. This approach can be used to pseudo-color surfaces, streamlines, glyphs, and animation characters. Additional parameter control is possible through variables in the shading process. Examples include mapping different reflectivity coefficients, such as specular and diffuse, to uncertainty values in order to alter the appearance of the visualization primitive. Another example would be manipulation of surface normals, similar to bump mapping, and in combination with lighting controls to provide indications of uncertainty [PA95].

Below are some examples that illustrate how modifying attributes can be used to incorporate uncertainty. For comparing the difference between the radiosities on a surface resulting from two different methods of form factor calculations, material properties of the polygon can be altered to make it either more or less diffuse or specular according to the difference on the polygon. For example, differences can be scaled to range from 0 to 1, and then mapped as diffuse and specular coefficients, such that the polygon with the least difference is assigned diffuse and

specular coefficients of 0, and the one with the largest difference is assigned coefficients of 1. Fig. 14 illustrates how mapping differences to diffuse coefficients will make those surface patches with higher differences appear brighter. Fig. 15 maps differences to specular coefficients. Note that the surfaces are rendered in connection with a movable light source. If the light source is tied to the camera or eye position, then altering specular coefficients allows one to focus on planes parallel to the viewing plane. Altering the specular coefficients is a better tool if the user is interested in viewing a particular area but altering the diffuse coefficients is better for viewing the error associated with the entire image.



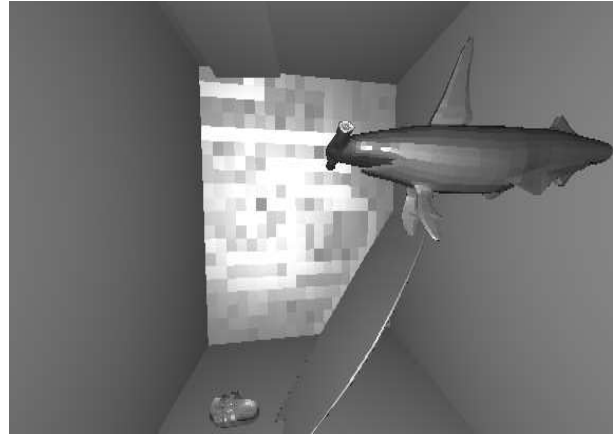Figure 14: Altering diffuse coefficients according to difference.



Figure 15: Altering specular coefficients according to difference.

Aside from the use of shading, lighting, and coloring parameters to alter the attributes, and hence, the appearance of visualization primitives for uncertainty visualization, embellishments such as textures can also be used to combine uncertainty information in visualization products. Using the same data set, Figs. 16 and 17 illustrate how the differences can be mapped to 2D and 3D textures respectively. Each surface patch in the scene is texture mapped with either a 2D circular pattern or a 3D conical shape. Where the differences are smaller, several smaller circles (or solid textures) are mapped; and where the differences are larger, larger circles or portions of circles (or solid textures) appear.
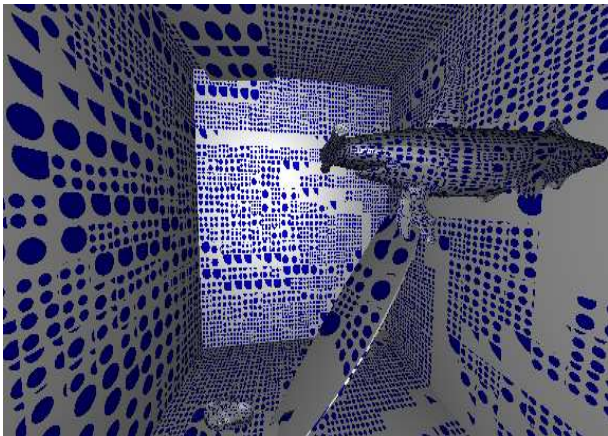


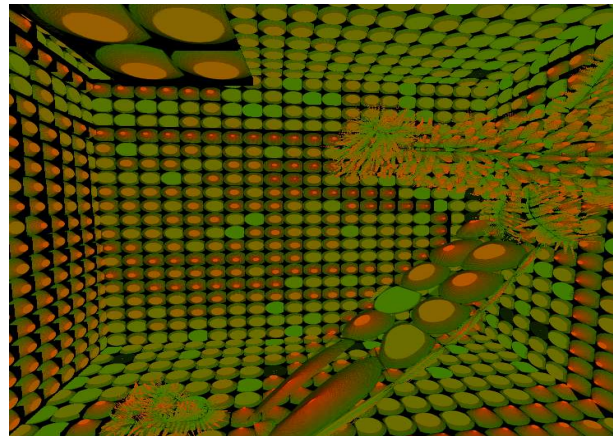Figure 16: Radiosity differences mapped to 2D circular textures.



Figure 17: Radiosity differences mapped to 3D solid textures.

For comparing simulated and real animations, a gridded mesh is placed over the 2D animation data. A normal coming out of the mesh plane at each grid point is then perturbed based on its distance from key points and their positional errors. Using Euclidean distances, the positional errors are calculated and used to perturb the mesh normals. Fig. 18 illustrates this technique.

For interpolation of vector data with magnitude and directional uncertainties, Fig. 19 uses pseudo-coloring to map the magnitude uncertainties to arrow glyph colors, and angular uncertainty to the background field.
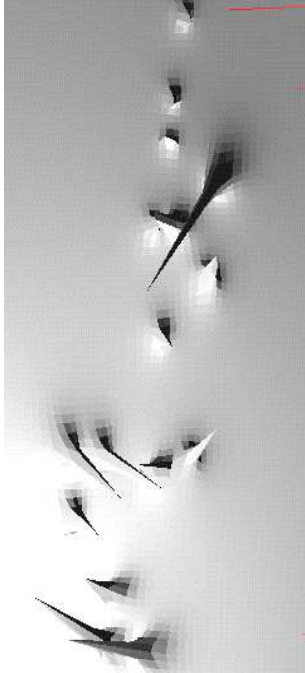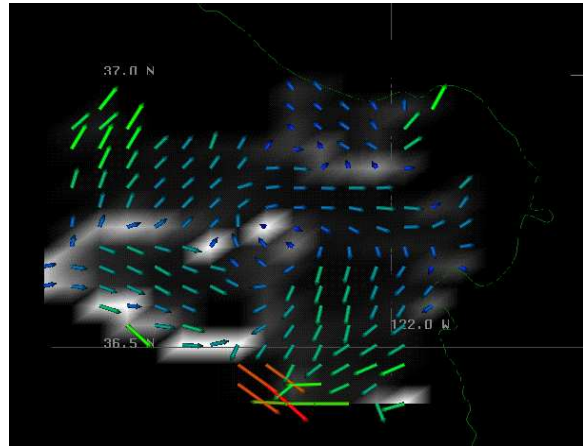


Figure 19: Ocean currents in are shown with arrow glyphs whose colors are mapped to the magnitude uncertainty. Background field indicates angular uncertainty.

Figure 18: Vertex normals of mesh points are bump mapped in the direction of local sampled error.

## 3.5   Animation

Animation, as a general approach for visualizing uncertainty, is applicable to most applications, including comparison of animation data and techniques. Uncertainty information can be visualized by mapping them to animation parameters such as: speed or duration, motion blur, range or extent of motion. We describe how animation is used for uncertainty visualization in the context of our application domains.

For comparing surface radiosities, animation is used together with geometry modification (translation and rotation). There are two possible mappings. The first (amplitude mapping) is to translate or rotate the surface patches proportional to the differences on each patch. All the patches are then animated in synchrony from their original position (and orientation) to their maximum translated position (and rotated orientation). This gives an undulating motion where the extent of motion or rotation is proportional to uncertainty. The second mapping (frequency mapping) is to assign a fixed translation or rotation amount to all surface patches. These are then animated in varying frequencies proportional to the differences on each patch. This gives a more confusing animation, but the viewer's attention is more easily drawn to fast moving patches. Depth perception using both methods of animating surface patches in 3D are enhanced with the aid of stereo glasses (e.g. Crystal Eyes).

Several animation techniques can also be used for comparing animation data. Examples that we have used to indicate uncertainty include random motion perturbation, motion blurring, and particle systems. Fig. 20 shows particles being generated, traced, and aged from key points in the human motion data. Initially a set of particles are randomly distributed around the key points. The subsequent positions, velocities, and accelerations were calculated by gravitationally attracting them towards their matching key points. Fig. 21 shows how motion blurring can be used to indicate the range of motion paths between two path interpolation methods (linear and cubic) over a 2D M-shaped set of key points.
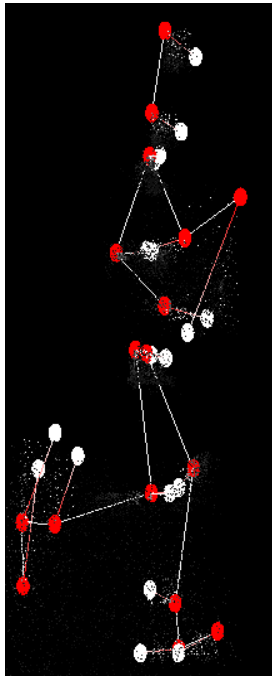




Figure 21: Animation with motion blurring to indicate uncertainty.

Figure 20: Particles are used to trace out the path of each joint.

For surface interpolation, animation is combined with other methods such as fat surfaces and glyphs. Specifically, fat surfaces are made to oscillate between their extents. The animation gives an impression of a thin surface growing thicker, and then thinner. Regions where the surface appears to grow thick very rapidly catch the user's attention and are indicative of places of greater differences. Alternatively, glyphs can be added and removed randomly to give a lively presentation of surface differences. Areas where the differences are larger will have proportionately more activity than areas with smaller differences.

For flow visualization, we introduce two ways of using animation to present differences in streamlines. Glyphs along the streamlines can be animated as the particle is advected along its path. An even more interesting animation is to rank or order the animation according to some user specified criteria, such as highest to lowest uncertainty. By presenting the difference information in this manner, the user is immediately alerted to the areas of high inaccuracy. This technique also identifies areas of equal uncertainty that are spatially apart quite well by presenting them immediately one after one another. Fig. 22 is a snapshot using such an animation method.

Animation can also be used to present the uncertainty information from the viewpoint of a particle traveling along a streamline. Actually, the viewpoint is taken from the midpoint between two streamlines. To understand this, imagine yourself being a particle traveling down the midpoint between two streamlines. As you go down the path, the extremities (from the two

calculated streamlines) will change in length and orientation. There are at least two alternative coordinate frames to use. One is to move and orient the local particle coordinate frame along the path trajectory. The other alternative is to simply translate the local particle coordinate frame within the world coordinate frame. That is, the frame mapping is achieved by translating the existing coordinate frame to the midpoint between the two streamlines at any given instant. This simplifies calculations and also helps the viewer orient themselves with respect to the world. Fig. 23 illustrates this method. This view is reminiscent of a twirling baton, hence the name. The longer the baton, the higher the uncertainty in streamline position. More twirling to the baton, the higher the uncertainty in the orientation.
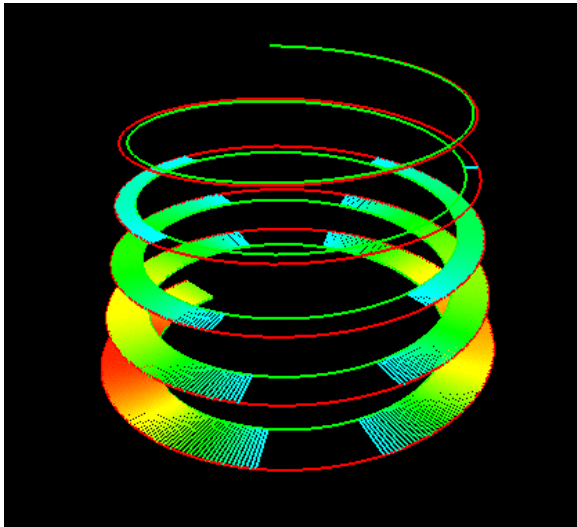


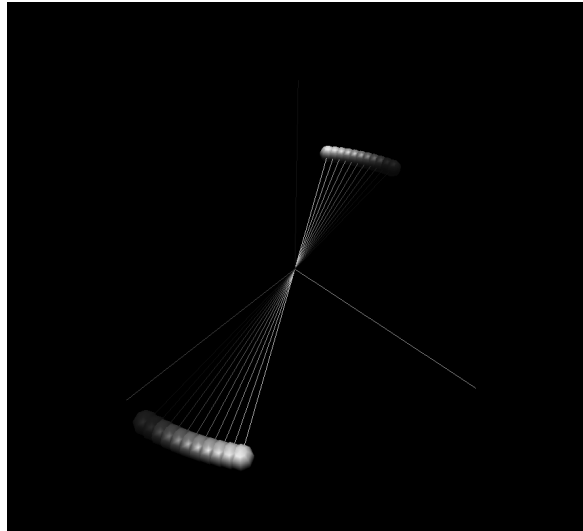Figure 22: Snapshot showing sections of streamlines with the same or higher differences.



Figure 23: Twirling baton display of differences between two streamlines. Point of view of midpoint particle.

## 3.6  Sonification

Uncertainty can be examined by mapping uncertainty to sound. We have used sound in conjunction with visualization to identify uncertainty. Sonification can often provide information about data that cannot be seen using visualization. Sound can enhance a graphical presentation by providing information about features of the data that may be hidden or occluded. Sound can also help the user to distinguish the size relationships between objects that may be difficult to determine visually because of projection distortion. In multivariate mappings, where visual clutter can destroy the usefulness of the display, the addition of sound can provide relief for the overloaded visual channel by allowing some variables to be presented aurally. Also, sound can provide redundancy of representation and allow data validation. An excellent discussion of additional benefits of auditory display in conjunction with other displays can be found in [Kra94, MF95].

We have explored the use of sonification in visualizing uncertainty of flow visualization and surface interpolation using LISTEN [LWS96]. LISTEN is a data sonification system that allows interactive mapping of data to sound parameters such as pitch, duration, volume, and timbre. Here, we describe two examples of sonifying uncertainty together with animation. In the first example, a glyph was chosen to move along a desired path or curve in the surface interpolation application, and along a streamline in the flow visualization application. The size (height or the radius) of the glyph was mapped to uncertainty. However, in regions of low variations of uncertainty, it was difficult to visually distinguish the size of glyphs. Therefore, uncertainty was

mapped to duration thereby slowing the movement of the glyphs and prolonging the sound in regions of high uncertainty. In another example, two different uncertainty parameters such as the mean and Gaussian curvatures of two surface interpolants were mapped to the pitches of violin and drum respectively. This sonification was played in conjunction with the presentation of cross-hair glyphs, where the lengths of the cross-hairs were mapped to uncertainty in the mean and Gaussian curvatures. This overloading of multivariate uncertainty information to visual and aural cues helped in the understanding of the correlation between different uncertainty parameters.

## 3.7  Psycho-Visual Approaches

This is probably the least understood and exploited group of methods that can be used for uncertainty visualization, and visualization in general. Perhaps, the main reason is the difficulty of eliciting a consistent impression or response from the subjects.

We have experimented with two different methods that fall under this category: "stereo-pairs" and subliminal messages. With the aid of stereo glasses, a 3D stereo effect can be achieved by quickly alternating the presentation of left and right views to the left and right eyes. Using this technology, we may compare two slightly different images. The motivation behind this is to make parts of the picture blurry, while other parts of the picture clear. If the two images were identical, we would lose the 3D stereo effect, but would still see a clear picture. When this method was applied to comparing the radiosities on surface patches, we achieved the desired effect of varying degree of clarity and blurriness. However, it was difficult to use this method for an extended period of time as the visual system kept trying to resolve the conflicting information arriving at both eyes, thereby resulting in eye strain.

The idea behind the use of subliminal messages was to see if we can open an additional channel to send information to the user. To this end, we experimented with flashing textual messages in between screen refresh, as well as putting the messages in texture maps and wrapping them onto objects in the rendered scenes. The textual messages (e.g. `itchy` and `sneeze`) were meant to evoke immediate response from the viewers. Based on our very limited experimentation, we were not able to get a repeatable and consistent set of responses.

While the findings in these two methods indicate some difficulties that still need to be resolved, we think that psycho-visual approaches have great potential and need to be explored further.

## 3.8  Summary

We have introduced a number of new methods for uncertainty visualization as presented in Table 4. These methods are grouped using the characteristics from Table 1, and presented in Table 5. From here, we can see that there is demand for research in techniques for vector and tensor visualization, and that we have added techniques for discrete and continuous visualization extents.

From our exploration of uncertainty visualization techniques, we have found that continuous visualization extents are more challenging than discrete visualization techniques. We believe that our grouping of methods into add glyph, add geometry, modify geometry, modify attributes, etc. is a powerful means to understanding the different methods. There are also many new techniques that are yet to be invented, but will likely fall into these categories.

In development of new techniques, it is important to evaluate them to determine if they are more effective than existing techniques. We have worked on evaluation methodologies, and have done a complete study of uncertainty glyphs. The new techniques that should survive are those that are shown to be effective in encoding, and easily decoded by users. The basic methodology, is to use visual tests where users examine visualizations, and decode the information within the graphic. The amount of error between the user interpretation and the encoding is statistically evaluated to determine if the visualizations are effective. There is a developed theory of speci-fiers, by Carswell [Car92], Cleveland [Cle85, CM86], and others which has shown that decoding

length is the most accurate, decoding area is less accurate, etc. Decoding of pseudo-colors, bump mapping, surface textures, etc. has not been shown to be straightforward yet. The evaluation of the effectiveness of new techniques is time consuming, but important, and we feel it is a wide open area for fundamental research in visualization.

In this section, we have presented a variety of tables that give different views of existing visualization methods, and that contrast these with our new methods. The emphasis has been to enumerate the state of the art as it exists, to clearly show what work needs to be done, and to demarcate our contribution. The variety of uncertainty visualization techniques we have illustrated in the images in this section show that there are more sophisticated methods than side by side comparison techniques, or ignoring the uncertainty altogether. A very sophisticated user may not need a visualization at all to understand a system under analysis, but visualization is for exploration of systems that we do not fully understand, and characterizing the uncertainty visually helps in more complete understanding.

| Value | Visualization Extent | |
|---|---|---|
| | discrete | continuous |
| scalar | glyphs (spheres, lines) | fat surfaces, displacement, affine transformations, magnitude/frequency, left/right, subliminal, and multivariate methods below |
| multivariate | glyphs (ellipsoids) IFS, batons | material property, ribbons, texture and bump mapping, oscillate, ranking, batons |
| vector | uncertainty glyphs | snow angel |
| tensor | | |

Table 5: New methods for uncertainty visualization and areas for further research

# 4    Conclusions

In this paper, a wide variety of new uncertainty visualization methods were introduced (adding glyphs, adding geometry, modifying attributes, modifying geometry, animation, sonification, and psycho-visual) and applied to many applications. The results of our research show there is a tremendous variety of possible means to map uncertainty into a scene. The complexity and hard work in deriving and understanding the uncertainty in the first place remains, but hopefully we have demonstrated tools that may be helpful to more easily investigate uncertainty. The approach of verity visualization where the technique for encoding the uncertainty is unambiguous, such as height glyphs for surface errors is not possible in all cases. The resultant data overloading provides more of a burden on the end user, but the critical nature of using data uncertainty while doing data analysis can be aided using our techniques.

We have done psycho-visual experiments for some of our approaches, and are working on developing evaluations for our other techniques as well. The resulting visualizations of data and uncertainty are integrated and present an accurate depiction to the user. We also found that more than one uncertainty method can be used together, and that application specific methods are relatively easy to generalize and be applied to different applications. Working with different applications has allowed us to design uncertainty visualization methods that would not have been otherwise apparent. As such, our current research efforts include:

1. Comparative visualization of experimental and simulated data for validation purposes.

2. 4D data assimilation and ensemble forecasting to resolve measurement and forecast differences.

3. Extension of the uncertainty computation and visualization from structured grids to scattered data sets, where the uncertainties are expected to be even more pronounced and important in data interpretation.

4. Investigation of volume rendering methods for the purpose of designing comparative 3D volume visualization methods. We plan to extend our work on 3D surface comparison methods to 3D volume comparison methods and apply these to 3D volume rendered scenes and images.

5. Development of techniques for comparing 2D images. The application domain of 2D images is large (e.g. compression algorithms, GIS, cartography, etc.) and work in this area can be of potential significance.

We believe that these uncertainty visualization methods will prove valuable to people who need to make informed decisions based on imperfect data.

# 5   Acknowledgements

# References

[ATS94]    James Arvo, Kenneth Torrance, and Brian Smits. A framework for the analysis of error in global illumination algorithms. In *Proceedings SIGGRAPH*, pages 75–84, Orlando, FL, July 1994. ACM SIGGRAPH.

[BBC91]    M. Kate Beard, Barbara P. Buttenfield, and Sarah B. Clapham. NCGIA research initiative 7: Visualization of spatial data quality. Technical Paper 91-26, National Center for Geographic Information and Analysis, October 1991.

[BCE$^+$92]   Ken W. Brodlie, Lesley Carpenter, Rae A. Earnshaw, Julian R. Gallop, Roger J. Hubbold, Anne M. Mumford, Chris D. Osland, and Peter Quarendon, editors. *Scientific Visualization: Techniques and Applications*, chapter on Visualization Techniques, pages 37–85. Springer-Verlag, 1992.

[BG89]     R. G. Bergeron and G. G. Grinstein. A reference model for the visualization of multi-dimensional data. In *Proceedings of Eurographics*, pages 393–399. Elsevier Science Publsihers, 1989.

[BHR$^+$94]   Manfred Brill, Hans Hagen, Hans-Christian Rodrian, Wladimir Djatschin, and Stanislav V. Klimenko. Streamball techniques for flow visualization. In *Proceedings: Visualization '94*, pages 225–231. IEEE Computer Society, 1994.

[Bri84]    D. R. Brillinger, editor. *The Collected Works of John W. Tukey*. Wadsworth and Brooks, 1984.

[Car92]    C. Melody Carswell. Choosing specifiers: An evaluation of the basic tasks model of graphical perception. *Human Factors*, 34(5):535–554, October 1992.

[CBB91]    Elizabeth Cluff, Robert Burton, and William Barrett. A survey and characterization of multidimensional presentation techniques. *Journal of Imaging Technology*, 17(4), 1991.

[Cha83]    Christopher Chatfield. *Statistics for Technology, A Course In Applied Statistics*. Chapman and Hall, third edition, 1983.

[Cle85]    William S. Cleveland. *The Elements of Graphing Data*. Wadsworth, 1985.

[CM86]    William S. Cleveland and Robert McGill. An experiment in graphical perception. *International Journal of Man-Machine Studies*, 25(5):491–500, November 1986.

[DH93]    T. Delmarcelle and L. Hesselink. Visualizing second-order tensor fields with hyper-streamlines. *IEEE Computer Graphics and Applications*, 13(4):25–33, July 1993.

[DH96]    D.L. Darmofal and R. Haimes. An analysis of 3d particle path integration algorithms. *Journal of Computational Physics*, 123(1):182–195, January 1996.

[dLvW93]    Willem C. de Leeuw and Jarke J. van Wijk. A probe for local flow field visualization. In *Proceedings of Visualization 93*, pages 39–45. IEEE Computer Society Press, October 1993.

[Far88]    Gerald Farin. *Curves and Surfaces for Computer Aided Geometric Design: A Practical Guide*. Academic Press, 88.

[FC95]    L. K. Forssell and S. D. Cohen. Using line integral convolution for flow visualization: curvilinear grids, variable-speed animation, and unsteady flows. *IEEE Transactions on Visualization and Computer Graphics*, 1(2):133–141, June 1995.

[Fis94]    P. Fisher. *Visualization in Geographical Information Systems*, chapter on Animation and Sound for the Visualization of Uncertain Spatial Information, pages 181–185. 1994.

[Ger92]    Nahum D. Gershon. Visualization of fuzzy data using generalized animation. In *Proceedings of Visualization 92*, pages 268–273. IEEE Computer Society Press, October 1992.

[GK94]    Ned Greene and Michael Kass. Error-bounded antialiased rendering of complex environments. In *Proceedings SIGGRAPH*, pages 59–66, Orlando, FL, July 1994. ACM SIGGRAPH.

[GU95]    A. Globus and S. Uselton. Evaluation of visualization software. *Computer Graphics*, pages 41–44, May 1995.

[HDD+94]    Hugues Hoppe, Tony DeRose, Tom Duchamp, Mark Halstead, Hugert Jin, John McDonald, Jean Schweitzer, and Werner Stuetzle. Piecewise smooth surface reconstruction. In *Proceedings SIGGRAPH*, pages 295–303, Orlando, FL, July 1994. ACM SIGGRAPH.

[HHS+92]    Hans Hagen, Stefanie Hahmann, Thomas Schreiber, Yasuo Nakajima, Burkard Wordenweber, and Petra Hollemann-Grundstedt. Surface interrogation algorithms. *IEEE Computer Graphics and Applications*, 12(5):53–60, September 1992.

[HPvW94]    L. Hesselink, F. Post, and J.J. van Wijk. Research issues in vector and tensor field visualization. *IEEE Computer Graphics and Applications*, 14(2):76–79, March 1994.

[ID90]    A. Inselberg and B. Dimsdale. Parallel coordinates: a tool for visualizing multidimensional geometry. In *Proceedings of Visualization'90*, pages 361–378. IEEE, October 1990.

[Ins85]    A. Inselberg. The plane with parallel coordinates. *The Visual Computer*, 1(1):69–91, 1985.

[KK93]    Peter Keller and Mary Keller. *Visual Cues: Practical Data Visualization*. IEEE Computer Society Press, 1993.

[Kra94]    G. Kramer. An introduction to auditory display. In Gregory Kramer, editor, *Auditory Display, Sonification, Audification, and Auditory Interfaces*, pages 1–78. Addison-Wesley, 1994.

[LC87]     W. E. Lorensen and H. E. Cline. Marching cubes: A high resolution 3D surface construction algorithm. *Computer Graphics*, 21(4):163 – 169, 1987.

[Lod96]    S. K. Lodha. Scattered data techniques for surfaces. In I. Chakravarty and D. Silver, editors, *Geometry Detection, estimation and Synthesis for Scientific Visualization*, page to appear. Academic Press, 1996.

[LPSW96]   Suresh K. Lodha, Alex Pang, Robert E. Sheehan, and Craig M. Wittenbrink. UFLOW: Visualizing uncertainty in fluid flow. In *Proceedings of Visualization 96*, page to appear, October 1996.

[LSG94]    Dani Lischinski, Brian Smits, and Donald P. Greenberg. Bounds and error estimates for radiosity. In *Proceedings SIGGRAPH*, pages 67–74, Orlando, FL, July 1994. ACM SIGGRAPH.

[LSPW96]   Suresh K. Lodha, Bob Sheehan, Alex T. Pang, and Craig M. Wittenbrink. Visualizing geometric uncertainty of surface interpolants. *Proceedings of Graphics Interface*, pages 238–245, May 1996.

[LWS96]    S. K. Lodha, C. M. Wilson, and R. E. Sheehan. LISTEN: sounding uncertainty visualization. In *Proceedings of Visualization 96*. IEEE, 1996.

[MF95]     R. Minghim and A.R. Forrest. An illustrated analysis of sonification for scientific visualization. In *Proceedings of Visualization 95*, pages 110–117. IEEE, 1995.

[MM94]     J.F. Moreno and J. Melia. An optimum interpolation method applied to the resampling of NOAA AVHRR data. *IEEE Transactions on Geoscience and Remote Sensing*, 32(1):131–151, January 1994.

[MMMY96]   Torsten Moller, Raghu Machiraju, Klaus Mueller, and Roni Yagel. Classification and local error estimation of interpolation and derivative filters for volume rendering. In *Proceedings Volume Visualization*, page to appear, San Francisco, CA, October 1996. IEEE.

[PA95]     Alex Pang and Naim Alper. Bump mapped vector fields. In *SPIE & IS&T Conference Proceedings on Electronic Imaging, Vol. 2410: Visual Data Exploration and Analysis II*, pages 78–86, color plate page 205. SPIE, February 1995.

[PF96]     Alex Pang and Adam Freeman. Methods for comparing 3D surface attributes. In *SPIE Vol. 2656 Visual Data Exploration and Analysis III*, pages 58–64. SPIE, February 1996.

[PFN94]    Alex Pang, Jeff Furman, and Wendell Nuss. Data quality issues in visualization. In *SPIE Vol. 2178 Visual Data Exploration and Analysis*, pages 12–23. SPIE, February 1994.

[TB96]     Greg Turk and David Banks. Image-guided streamline placement. In *Proceedings SIGGRAPH*, pages 453–460, New Orleans, LA, August 1996. ACM SIGGRAPH.

[TK93]     Barry N. Taylor and Chris E. Kuyatt. Guidelines for evaluating and expressing the uncertainty of NIST measurement results. Technical report, National Institute of Standards and Technology Technical Note 1297, Gaithersburg, MD, January 1993.

[Tuf83]    Edward R. Tufte. *The Visual Display of Quantitative Information*. Graphics Press, 1983.

[Tuf90]    Edward R. Tufte. *Envisioning Information*. Graphics Press, 1990.

[Tuk77]    John W. Tukey. *Exploratory Data Analysis*. Addison Wesley, 1977.

[UH90]     J.K. Udupa and H.-M. Hung. Surface versus volume rendering: a comparative assessment. In *Proceedings of the First Conference on Visualization in Biomedical Computing*, pages 83–91, Atlanta, GA, May 1990. IEEE Comput. Soc.

[VGW94]   Allen Van Gelder and Jane Wilhelms. Topological considerations in isosurface generation. *ACM Transactions on Graphics*, 13(4), October 1994. Also UCSC technical report UCSC-CRL-90-14.

[Wit95]   Craig M. Wittenbrink. IFS fractal interpolation for 2D and 3D visualization. In *IEEE Visualization '95*, pages 77–84, Atlanta, GA, November 1995. IEEE.

[WPL95]   Craig M. Wittenbrink, Alex T. Pang, and Suresh Lodha. Verity visualization: Visual mappings. Technical Report UCSC-CRL-95-48, Univ. of Cal. Santa Cruz, 1995.

[WPL96]   Craig M. Wittenbrink, Alex T. Pang, and Suresh K. Lodha. Glyphs for visualizing uncertainty in vector fields. *IEEE Transactions on Visualization and Computer Graphics*, September 1996. to appear.

[WSF+95]   Craig M. Wittenbrink, Elijah Saxon, Jeff J. Furman, Alex T. Pang, and Suresh Lodha. Glyphs for visualizing uncertainty in environmental vector fields. In *Vol. 2410 SPIE & IS&T Conference Proceedings on Electronic Imaging: Visual Data Exploration and Analysis*, pages 87–100. SPIE, February 1995.